Utilization of Bayesian Framework in Lithology and Fluid Prediction by Using Inverted Elastic Parameter from Seismic Data

Rizky Adityo Prastama[1,*] and Ignatius Sonny Winardhi[1]

[1]Institut Teknologi Bandung
*Email: p.rizkyadityo@gmail.com

Abstract: Development stage of a hydrocarbon field usually aims to discover additional reserves within the working area. In this stage, more data, such as well log and core sample, are available to be included in the development plan compared to early exploration stage. Incorporating the information from well to know the distribution of the prospective zone could be done in many ways. In this paper, the workflow of how information in producing well is utilized to predict the distribution of gas-filled sand by using Bayesian framework is presented. Bayesian frameworks use prior statistical information of the gas sand itself, such as prior probability and likelihood function, in calculating the posterior probability. From the available well data, three lithology and its fluid content are classified as gas sand, brine sand, and shale. The likelihood function of these lithology is computed using Gaussian distribution and the prior probability is estimated by Markov-chain approach. Based on the prior information, the posterior probability is iteratively calculated by using values from elastic parameter section that is inverted from seismic data. The resulting probability section of each lithology will have value ranging from 0 to 1. The maximum-a-posteriori (MAP) in every location in the section is concluded as the most probable lithology to be discovered. The result shows that the distribution of gas sand can be predicted quite well by using acoustic impedance and Vp/Vs ratio. This is proven by a good fit between the predicted lithology section and the well.
Keywords: Bayesian, posterior probability, likelihood, prediction, lithology

Abstrak: Tahap pengembangan dari lapangan hidrokarbon umumnya bertujuan untuk menemukan cadangan tambahan di dalam area kerja yang dimiliki. Pada tahap ini, lebih banyak data, seperti data log sumur dan data *core*, yang bisa digunakan untuk rencana pengembangan dibandingkan pada tahap eksplorasi awal. Penggabungan informasi dari sumur untuk mengetahui sebaran dari zona prospek dapat dilakukan dengan banyak cara. Pada tulisan ini, akan ditampilkan alur kerja dimana informasi dari sumur produksi dapat digunakan dalam memprediksi sebaran batupasir berisi gas dengan menggunakan kerangka kerja Bayesian. Kerangka kerja Bayesian menggunakan informasi statistik awal (*prior*) dari batupasir berisi gas itu sendiri, seperti probabilitas awal dan fungsi kemungkinan (*likelihood*), dalam menghitung probabilitas *posterior*. Dari data sumur yang tersedia, tiga litologi beserta konten fluida diklasifikasikan sebagai batupasir gas, batupasir *brine*, dan batulempung. Fungsi *likelihood* dari ketiga litologi tersebut dihitung menggunakan distribusi Gauss dan probabilitas awal diestimasi menggunakan pendekatan rantai Markov. Berdasarkan informasi awal tersebut, probabilitas *posterior* secara iteratif dihitung berdasarkan nilai parameter elastik yang diperoleh dari inversi data seismik. Penampang probabilitas setiap litologi yang dihasilkan memiliki rentang nilai antara 0 sampai 1. Nilai *maximum-a-posteriori* (MAP) pada setiap lokasi di penampang tersebut disimpulkan sebagai litologi yang paling mungkin untuk ditemukan. Hasil yang diperoleh menunjukkan bahwa distribusi batupasir berisi gas dapat diprediksi dengan cukup baik ketika menggunakan impedansi akustik serta rasio Vp/Vs. Hal ini dibuktikan dengan kecocokan yang cukup baik antara penampang prediksi litologi dengan sumur.
Kata kunci: Bayesian, probabilitas posterior, kemungkinan, prediksi, litologi

1 INTRODUCTION

The advanced stage of hydrocarbon field analysis is to expand and develop the operation to retrieve more reserves. Development plan is usually constructed from available data such as well logs and seismic. The goal is to find another possible hydrocarbon accumulation area that might be related to the current production well. The physical characteristics of the pay zone in the production well is analyzed and the distribution is mainly assessed by using the seismic data.

Seismic data primarily give initial information of geological structure inside the coverage area. When a well is drilled, it enhances the use of seismic data to be inverted into elastic parameters such as acoustic impedance and Vp/Vs ratio. These elastic parameters are commonly used to describe the properties of rock along with its fluid content. Once the elastic parameter section or volume from seismic data is obtained, the lateral distribution of pay zone can be analyzed.

However, it is widely known that seismic data is very prone to noise. It can be recorded from the data acquisition and remains in the post-processing stages. This can lead to inaccurate inverted elastic parameters. The resulting elastic parameter could be misleadingly affected by noise. Other

than that, the physical characteristic of rock is a continuous value. It means that there is no single exact value that represent a lithology. For example, a carbonate rock p-wave velocity (Vp) lies between 3000 m/s up to 6500 m/s (Kahraman & Yeken, 2008). The exact value is controlled by mineral composition, total porosity, pore type, fluid content, pressure, etc (Xu & Payne, 2009). This gives us an idea that if we obtain a Vp that falls into that range, it is very likely to be a carbonate rock. Based on this perspective, prediction of lithology and fluid content from elastic parameter could not be seen as a deterministic approach. This is where probabilistic point of view should be considered in lithology prediction. One natural choice of probabilistic framework that includes continuous likelihood value is Bayesian (Buland, Kolbjørnsen, Hauge, Skjæveland, & Duffaut, 2008; Grana & Rossa, 2010; Zhao, Geng, Cheng, hua Han, & Guo, 2014).

In this paper, we are going to present the full workflow of lithology and fluid content (LFC) prediction by combining simultaneous inversion and Bayesian framework. The workflow begins with cross-plot analysis to understand the behavior of our target zone, which is a gas-filled sand reservoir. The best elastic parameters that can separate the gas sand from other observed lithology is chosen. The available seismic data is then inverted to get these elastic parameters section. Finally, Bayesian framework is used to iteratively calculate the probability of gas sand in every point in the given elastic parameters section. By using this approach, we are also calculating the uncertainty to find gas sand in any given point in subsurface.

2   METHODOLOGY

We are going to use single reference or training well for prior analysis of the gas sand and one section of seismic to predict the lateral distribution of the gas sand itself. Since the well has very limited data, our focus in this paper is to show the workflow of how to utilize Bayesian framework and benefit us in adding layers of analysis in field development.

2.1   Bayesian Posterior Probability

Bayesian posterior probability is a conditional probability of an event based on given data or evidence. In our case, it is a probability of an LFC based on some elastic parameter that is observed. We can write the Bayesian posterior probability as follows:

$$P(L \mid m) = \frac{P(m \mid L)P(L)}{P(m)} \tag{1}$$

where $P(m \mid L)$ is the likelihood function while P(L) and P(m) are prior probability of the LFC and the elastic parameter respectively. The idea of this approach is every defined LFC that we are going to predict already have a prior probability p(L). When the evidence emerges, such as the inverted elastic parameter value from seismic data, this prior probability is updated by the likelihood function $P(m \mid L)$ and become posterior probability. The likelihood function itself is a function that estimate how likely elastic parameter value m is related to LFC L. For example, suppose

we get a data somewhere in subsurface where the p-wave velocity is 2500 m/s. We can say that, based on this p-wave value, we are more likely to find shale compared to carbonate. The mathematical expression for this case is the value of $P(m = 2500m/s \mid L = "shale")$ is bigger when compared to the $P(m = 2500m/s \mid L = "Carbonate")$.

It is common to use more than one elastic parameter for predicting the LFC. Ideally, we can use two elastic parameters because we usually perform cross-plot analysis between two parameters that work best in separating different LFC in our area of interest. Additional elastic parameter also works as a constraint to reduce the ambiguity of single elastic parameter. When we use two elastic parameters (m_1 and m_2), the formulation of Bayesian posterior probability above can be modified as follows:

$$P(L \mid m_1, m_2) = \frac{P(m_1, m_2 \mid L)P(L)}{P(m_1, m_2)} \tag{2}$$

The conditional independence theorem states that $P(A, B \mid C) = P(A \mid C)P(B \mid C)$. We can rewrite equation above to:

$$P(L \mid m_1, m_2) = \frac{P(m_1 \mid L)P(m_2 \mid L)P(L)}{P(m_1, m_2)} \tag{3}$$

The denominator P(m_1, m_2) is acting as a normalizing factor. The posterior probability is then proportional to (Zhao et al., 2014):

$$P(L \mid m_1, m_2) \propto P(m_1 \mid L)P(m_2 \mid L)P(L) \tag{4}$$

The elastic parameters (m_1 and m_2) are continuous value. We can use Gaussian likelihood distribution for both $P(m_1 \mid L)$ and $P(m_2 \mid L)$. For prior probability of LFC P(L), we will use Markov-chain approach.

2.2   Gaussian Likelihood Distribution

Gaussian distribution, or normal distribution, is a type of continuous probability distribution of a variable that is centred on its mean with the curve width defined by its standard deviation. It can be written as:

$$P(m = x \mid L) = f(x) = \frac{1}{\sigma\sqrt{2\pi}}e^{\frac{1}{2}(\frac{x-\mu}{\sigma})^2} \tag{5}$$

where x is the variable, μ is the mean, and σ is the standard deviation. To get the likelihood function of an elastic parameter m, we need to get the cluster of data from cross-plot analysis that we can classify it as LFC L. This set of data is then calculated for its mean and standard deviation so that we can create the likelihood function following the above equation. After we create the likelihood function, whenever we have a random value of m, we can calculate its likelihood for LFC L.

2.3   Markov-chain Prior Probability

The final aspect of Bayesian posterior probability that we need to calculate is the prior probability of the LFC. Prior probability itself is the initial chance, without any evidence

or data, to get the LFC at any place below the surface. The Markov-chain approach is chosen because it is quite related to how sedimentary rock sequence is formed.

Markov-chain is a series of events where the probability of the upcoming event is only determined by the current event. We can write it mathematically as follows:

$$P(L_i) = \prod_t |P(L_i \mid L_{i-1}) \qquad (6)$$

Where L_i is the LFC at depth point i and L_{i-1} is the LFC right beneath it. The reason why Markov-chain is a good approach in geological observations, such as stratigraphic sequences of lithologic units, is because the lithologic units can be structured as discrete events that are spaced equally along vertical axis (Krumbein & Dacey, 1969). The transition between unit is represented by using transition matrix. Suppose we have two lithologic units in our well named A and B. To create the transition matrix, we should count the transition between A to A, A to B, B to A, and B to B in upward or downward direction. Below is the example of the transition matrix representing lithologic unit A and B:

$$T = \begin{pmatrix} : & A & B \\ A & 30/50 & 20/50 \\ B & 05/20 & 15/20 \end{pmatrix} = \begin{pmatrix} : & A & B \\ A & 0.60 & 0.40 \\ B & 0.25 & 0.75 \end{pmatrix} \qquad (7)$$

The transition matrix above shows that there are 50 transitions from unit A and 20 transition from unit B. Each element of the matrix represents how many transitions from each unit to another. If we look at the first row, there are 30 transitions from unit A to unit A again and another 20 transitions from unit A to unit B.

To estimate the prior probability, we should calculate for stationary condition of the transition matrix (Grana, Mukerji, Dvorkin, & Mavko, 2012; Larsen, Ulvmoen, Omre, & Buland, 2006). The stationary condition is reached when:

$$nT = n \qquad (8)$$

The variable n is a row matrix with n-number of columns depending on how many lithologic units we have in our data. In our example using two lithologic units above, we can define an initial condition with $n = [1\ 0]$ or $n = [0\ 1]$. We then substitute this matrix to equation 8 above to get a new matrix n. This process is done iteratively until the input matrix n on the left-side of the equation resulting the matrix n itself on the right-side. The final matrix n is representing the prior probability of each lithologic units.

2.4   Simultaneous Inversion

Hampson, Russell, and Bankhead (2005) proposed a method in inverting acoustic impedance, shear impedance, and density simultaneously from seismic data. The method assumes that reflectivity follows the Aki and Richards (2002) equation as a function of angle. Originally, the reflectivity in the interface between two different layers (here are labelled as layer 1 and 2) for normal incident wave where $\theta = 0^o$ is:

$$R_{p0} = \frac{Z_{p2} - Z_{p1}}{Z_{p2} + Z_{p1}} \approx \frac{1}{2}\frac{\triangle Z_p}{\overline{Z}_p} \approx \frac{1}{2}(\frac{\triangle V_p}{\overline{V}_p} + \frac{\triangle \rho}{\overline{\rho}}) \qquad (9)$$

$$R_{s0} = \frac{Z_{s2} - Z_{s1}}{Z_{s2} + Z_{s1}} \approx \frac{1}{2}\frac{\triangle Z_s}{\overline{Z}_s} \approx \frac{1}{2}(\frac{\triangle V_s}{\overline{V}_s} + \frac{\triangle \rho}{\overline{\rho}}) \qquad (10)$$

$$R_{\rho0} = \frac{\triangle \rho}{\overline{\rho}} \qquad (11)$$

where R_P0, R_S0, and $R_{\rho0}$ are reflectivity value that are caused by difference in acoustic impedance, shear impedance, and density, respectively (Simmons & Backus, 1996). Buland and Omre (2003) proposed an approximation for small reflectivity difference between two layers as follows:

$$R_{p0} = \frac{1}{2}\frac{\triangle Z_p}{\overline{Z}_p} = \frac{1}{2}\triangle ln Z_p = \frac{1}{2}(ln Z_{p_{i+1}} - ln Z_{p_i}) \qquad (12)$$

The index i in equation 12 is the label for each adjacent layer in different depth location. If we assume that there are N layers with their own elastic characteristic, equation 12 can be rewritten into matrix form as follows:

$$\begin{bmatrix} R_{p_1} \\ R_{p_2} \\ \vdots \\ R_{p_N} \end{bmatrix} = \frac{1}{2}\begin{bmatrix} -1 & 1 & 0 & \ldots \\ -1 & 1 & 0 & \ldots \\ -1 & 1 & 0 & \ldots \\ \vdots & \ddots & \ddots & \ddots \end{bmatrix}\begin{bmatrix} ln Z_{p_1} \\ ln Z_{p_2} \\ \vdots \\ ln Z_{p_N} \end{bmatrix} \qquad (13)$$

This is the reflectivity value based on the difference of P-impedance for normal incident wave. Since seismic trace (T) is a product between wavelet (W) and the reflectivity (R), the matrix form of convolution process involving these three variables is:

$$\begin{bmatrix} T_1 \\ T_2 \\ \vdots \\ T_N \end{bmatrix} = \begin{bmatrix} w_1 & 0 & 0 & \ldots \\ w_2 & w_1 & 0 & \ldots \\ w_3 & w_2 & w_1 & \ldots \\ \vdots & \ddots & \ddots & \ddots \end{bmatrix}\begin{bmatrix} R_{p_1} \\ R_{p_2} \\ \vdots \\ R_{p_N} \end{bmatrix}$$

$$= \frac{1}{2}\begin{bmatrix} w_1 & 0 & 0 & \ldots \\ w_2 & w_1 & 0 & \ldots \\ w_3 & w_2 & w_1 & \ldots \\ \vdots & \ddots & \ddots & \ddots \end{bmatrix}\begin{bmatrix} -1 & 1 & 0 & \ldots \\ -1 & 1 & 0 & \ldots \\ -1 & 1 & 0 & \ldots \\ \vdots & \ddots & \ddots & \ddots \end{bmatrix}\begin{bmatrix} ln Z_{p_1} \\ ln Z_{p_2} \\ \vdots \\ ln Z_{p_N} \end{bmatrix} \qquad (14)$$

or can be simply written as:

$$T = \frac{1}{2}WD ln Z_p \qquad (15)$$

where D is called the derivative matrix. Fatti, Smith, Vail, Strauss, and Levitt (1994) simplified Aki-Richards equation by incorporating normal incident reflectivity to estimate the P-wave reflectivity as a function of angle θ.

$$R_p p(\theta) = c_1 R_{p0} + c_2 R_{s0} + c_3 R_{\rho0} \qquad (16)$$

where $c_1 = 1 + tan^2\theta$, $c_2 = -8\gamma^2 tan^2\theta$, $c_3 = -0.5 tan^2\theta + 2\gamma^2 sin^2\theta$, and $\gamma = \frac{V_s}{V_p}$. The inversion will use angle gather data or seismic trace as a function of angle. By

combining equation 15 and 16, the forward equation of trace T as a function of angle θ is

$$T(\theta) = \frac{1}{2}c_1 W(\theta) Dln(Z_p) + \frac{1}{2}c_2 W(\theta) Dln(Z_s) \\ + \frac{1}{2}c_3 W(\theta) Dln(\rho) \tag{17}$$

Hampson et al. (2005) described that the algorithm is working for natural logarithmic of impedance. The proposed method described the linearity between lnZ_p, lnZ_s, and $ln\rho$ as:

$$lnZ_s = kln(Z_p) + k_c + \triangle ln(Z_s) \tag{18}$$

$$ln\rho = mln(Z_p) + m_c + \triangle ln(\rho) \tag{19}$$

where k and m are gradients and k_c and m_c are intercepts. Equation 18 and 19 tell us that to invert shear impedance and density, the algorithm will use the deviation from the linear fit ($\triangle lnZ_s$ and $\triangle ln\rho$) of acoustic impedance. We can rewrite the equation 17 in matrix form as follows:

$$\begin{bmatrix} T(\theta_1) \\ T(\theta_2) \\ \vdots \\ T(\theta_N) \end{bmatrix} = \begin{bmatrix} \widetilde{c}_1(\theta_1)W(\theta_1)D & \widetilde{c}_2(\theta_1)W(\theta_1)D \\ \widetilde{c}_1(\theta_2)W(\theta_2)D & \widetilde{c}_2(\theta_2)W(\theta_2)D \\ \vdots & \vdots \\ \widetilde{c}_1(\theta_N)W(\theta_N)D & \widetilde{c}_2(\theta_N)W(\theta_N)D \end{bmatrix}$$
$$\begin{matrix} \widetilde{c}_3(\theta_1)W(\theta_1)D \\ \widetilde{c}_3(\theta_2)W(\theta_2)D \\ \vdots \\ \widetilde{c}_3(\theta_N)W(\theta_N)D \end{matrix} \begin{bmatrix} \ln Z_p \\ \triangle ln(Z_s) \\ ln(\rho) \end{bmatrix} \tag{20}$$

where $\widetilde{c}_1 = \frac{1}{2}c_1 + \frac{1}{2}kc_2 + m$ and $\widetilde{c}_2 = \frac{1}{2}c_2$. From the mathematical expressions mentioned above, it can be concluded that we need to define the wavelet for each angle ($W(\theta)$). Other than that, the proposed method is to create initial impedance model where $[ln(Z_p) \quad \triangle ln(Z_s) \quad \triangle ln(\rho)]^T = [ln(Z_{p0}) \quad 0 \quad 0]^T$ to cover the low frequency. The process is done iteratively by using conjugate gradient method to solve for Z_p, Z_s, and ρ.

3 RESULTS AND DISCUSSION

3.1 Prior Analysis in Training Well

Analyzing the elastic behavior of the LFC that we are going to predict is crucial. Our goal is to get two elastic parameters that can separate each LFC so that the prediction will be accurate. We can achieve this by using cross-plot analysis. Before we perform the analysis, Figure 1 is the complete log data in the target gas sand zone. In this study, our well data is limited to density, p-wave, and s-wave velocity. On the rightmost track, we can see the interpreted LFC based on the available log data. The magenta, yellow, and green are representing gas sand, brine sand, and shale, respectively. The LFC is interpreted from the available log data. We can see that the gas sand is mostly defined by decreasing bulk density and p-wave velocity compared to the brine sand. This is mainly because the fluid difference inside the pore
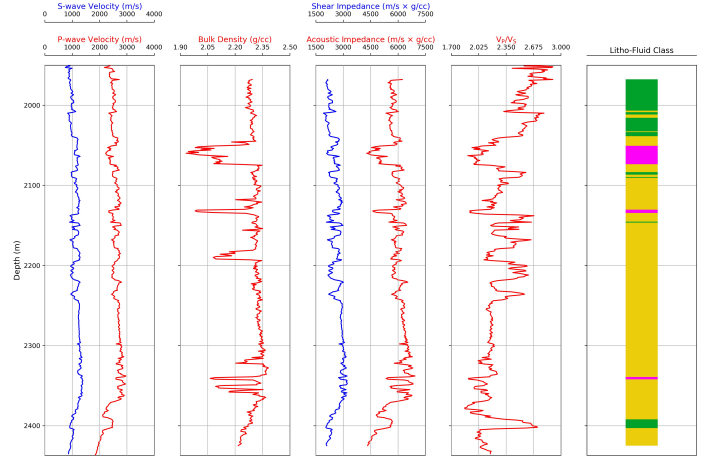
Figure 1. The available geophysical log data in training well. The rightmost track is the interpreted LFC. Magenta, yellow, and green are representing gas sand, brine sand, and shale, respectively.
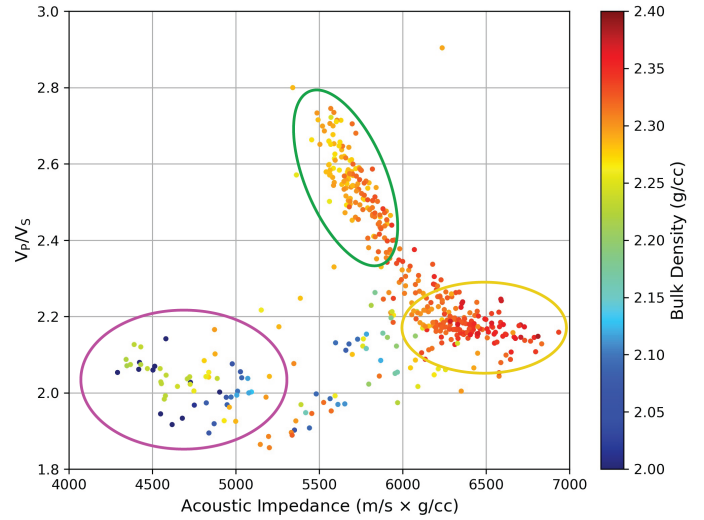
Figure 2. Cross-plot analysis between acoustic impedance and Vp/Vs ratio with bulk density as overlying color. The circles are cluster of each LFC where magenta, yellow, and green are for gas sand, brine sand, and shale, respectively.

since gas has lower density and bulk modulus compared to water, resulting in lower bulk density and p-wave velocity. We also use Vp/Vs ratio in the fourth track to see if there is shale in our area. It can be inferred that acoustic impedance and Vp/Vs ratio can separate LFCs. Figure 2 is the cross-plot between both elastic parameters.

The circles with same color code are the cluster of LFCs. The outcome of cross-plot analysis in our workflow is to get the mean μ and standard deviation σ of each LFC for calculating the Gaussian likelihood distribution. Both parameters can be calculated from every data point inside the cluster. Table 1 below is the mean and standard deviation for acoustic impedance and Vp/Vs ratio. Using these values and equation 5, we can set a range of acoustic impedance and Vp/Vs ratio value and create the visualization of the likelihood distribution (Figure 3).

Table 1. Mean and standard deviation of Acoustic Impedance(AI) and Vp/Vs ratio for each LFC based on the cross-plot analysis in Figure 2

LFC	AI Mean(μ)	AI Std. Dev(σ)	Vp/Vs Mean(μ)	Vp/Vs Std.Dev(σ)
Gas Sand	4725.38	226.71	2.03	0.06
Brine Sand	6346.04	182.23	2.18	0.05
Shale	5692.62	109.11	2.56	0.08
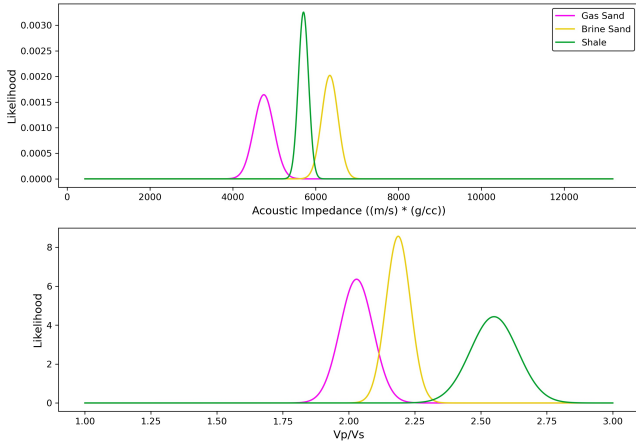
Figure 3. The Gaussian likelihood distribution of each LFC in both acoustic impedance (top) and Vp/Vs ratio (bottom). These distributions are constructed by substituting values from Table 1 into equation 5.

The distribution shows that acoustic impedance will be more sensitive in separating fluid content inside the sandstone. In equation 4, Bayesian framework use likelihood function for updating the prior believe or prior probability of each LFC and we call this updated probability as posterior probability. We can see in Figure 3 that in the range between 4000 to 5500 (m/s) * (g/cc), the likelihood of gas sand is reaching its maximum while the likelihood of other classes remains at 0. It means that when we observed acoustic impedance in this range, we are most likely to discover gas sand. This condition is the reason why we conclude that acoustic impedance is very sensitive in detecting fluid content inside the rock. Meanwhile, for Vp/Vs, the range below gas sand curve have some overlaps with brine sand (2.00 – 2.25). By using the same concept, if we get the Vp/Vs value in this range, there are two possible outcome which are gas sand or brine sand. We can conclude that Vp/Vs is not as sensitive as acoustic impedance in identifying fluid content. However, we can see the shale likelihood function (green curve) is well separated in the upper end of the Vp/Vs value. We can conclude Vp/Vs will give more contribution, or weight, in separating shale from sandstone.

The LFC track in Figure 1 can be used for estimating the prior probability of each LFC. In Figure 1, there are 457 transitions based on the interpreted LFC track. Since we defined three LFC, we use 3×3 transition matrix to map the number of transitions between every classes as shown below. The rows represent the initial lithology, and the columns represent the transition lithology. For example, we can see that there are 46 transitions from gas sand where 38 of them are transitioning into gas sand again right beneath it while the other 8 are into brine sand.

$$T = \begin{bmatrix} : & GS & BS & Sh \\ GS & 38 & 8 & 0 \\ BS & 8 & 254 & 11 \\ Sh & 0 & 12 & 126 \end{bmatrix} \quad (21)$$

To estimate the prior probability, first we need to normalize the transition matrix above as follows:

$$T = \begin{bmatrix} : & GS & BS & Sh \\ GS & 38/46 & 8/46 & 0/46 \\ BS & 8/273 & 254/273 & 11/273 \\ Sh & 0/138 & 12/138 & 126/138 \end{bmatrix}$$

$$= \begin{bmatrix} : & GS & BS & Sh \\ GS & 0.826 & 0.174 & 0 \\ BS & 0.029 & 0.930 & 0.041 \\ Sh & 0 & 0.087 & 0.913 \end{bmatrix} \quad (22)$$

Finally, we can estimate the prior probability of each class by finding the stationary condition of transition matrix above. The resulting row matrix, consisting of 3 elements for each class, is:

$$P(L) = \begin{bmatrix} 0.103 & 0.613 & 0.284 \end{bmatrix} \quad (23)$$

The prior probability matrix above shows that the probability for brine sand (second column) is very high with 61.3%. This is acceptable since we can see in Figure 1 that our area of study is dominated with brine-filled sand. Although the prior probability of gas sand is the lowest with 10.3%, we can expect that the final posterior probability will be updated based on the likelihood function of acoustic impedance and Vp/Vs ratio.

3.2 LFC Prediction Results

The elastic parameter sections (Figure 4) are our main information in estimating the posterior probability of each LFC laterally. These two sections are primarily a two-dimensional matrix with rows and columns. Each row represents the two-way-time (TWT) of the data while each column is assigned to specific CDP or coordinate. The algorithm takes the acoustic impedance and Vp/Vs ratio in each section and substitutes it to the likelihood function. This process is done iteratively for each LFC by multiplying the likelihood value and the LFC's prior probability itself. Figure 5 below are the posterior probability for gas sand, brine sand, and shale.

The results in Figure 5 show us that shale has higher probability to present in the upper part of the section while the lower part has higher probability of sandstone. The gas sand location is laterally accumulated in the middle of the section. To see the LFC distribution better, we can use the
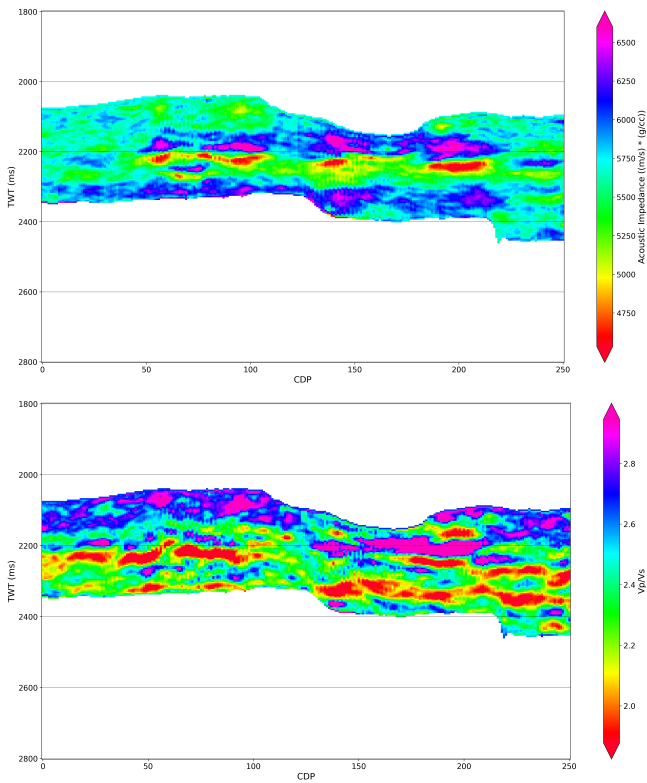
Figure 4. Simultaneous inversion results for acoustic impedance (top) and Vp/Vs ratio (bottom). High Vp/Vs ratio can be seen on upper part that might be related to shale meanwhile inferring sandstone, especially with gas, is harder just by seeing these two sections

Figure 5. Posterior probability results of gas sand (top), brine sand (middle), and shale (bottom). Red means highest probability of the LFC to be discovered in the given location below the surface

concept of maximum-a-posteriori (MAP). MAP is the maximum posterior probability value in every location in our section. In other words, this method choose which LFC has the higher posterior probability and infers it as the most probable outcome in every point in the section. Figure 6 is the MAP of the three posterior probability section that we obtained before.

We can see that the results in seismic section have a good fit with the well especially in the gas sand segment. The slight difference between the predicted lithology in the section and the interpreted lithology in inserted well could be caused by the limited amount of data as a constraint for interpreting the lithology in the well itself. The data that we use to interpret lithology are very limited to density, P-wave, and S-wave velocity log. Based on the cross-plot in Figure 2, the use of density log to identify gas sand is quite good since it is very distinctive compared to the other two classes. This is why we can have a good lateral continuity for gas sand. For the shale and brine sand, we mainly rely on acoustic impedance and Vp/Vs ratio which is generally not good enough for detecting clay content and the amount of water inside the pore. Therefore, in the lower part of the section, we still find some mismatch predictions between these two classes. However, the MAP section above shows the power of Bayesian posterior probability inference in predicting LFC by using seismic data. The distribution of each LFC is seen as a probability. This perspective will be very useful to de-

termine the future of development since we quantitatively estimating the uncertainty of our target.

Another aspect that we would like to discuss is the importance of accuracy in cross-plot analysis. The posterior probability section of each LFC is calculated primarily by using information from training well (P(m—L) and P(L)). The LFC interpretation in training well will determine the prior probability of each LFC itself while the LFC cluster definition in cross-plot affects the resulting likelihood distribution. To get a clearer image on this issue, Figure 7 below are sets of figures where we define the LFC cluster differently.

The key difference that should be noticed is how overlapping cluster will create more variation in posterior probability results. In earlier results, most part of the section is almost divided only to 0 or 1. Each LFC is very distin-
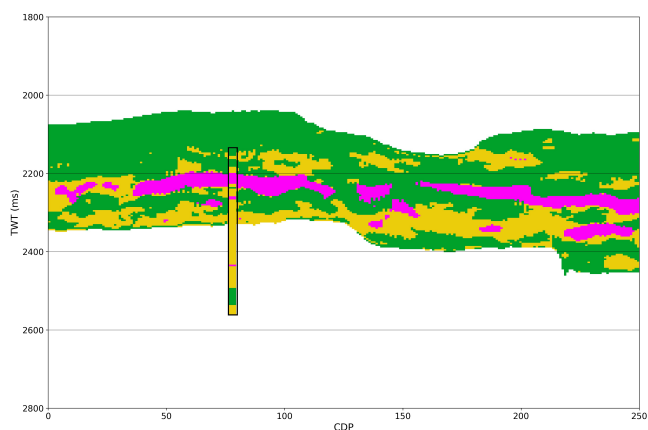
Figure 6. The predicted LFC based on maximum-a-posteriori (MAP) value. Notice that the gas sand (magenta) has a good agreement with the interpreted LFC in training well. It has another accumulation region in the right-hand side that could be the next prospect to be drilled
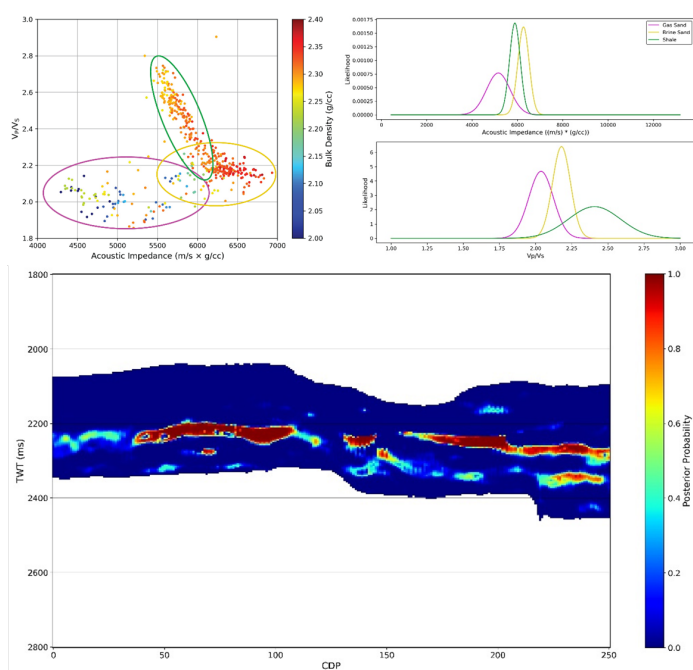
Figure 7. The new clusters of LFCs to test the overlapping effect (top left); Likelihood distribution (top right); The new posterior probability for gas sand (bottom).

guishable so that the posterior probability will be 1 when the necessary parameters fall into its acceptable range and 0 otherwise. Meanwhile, in Figure 7 above, overlapping caused more area with varying posterior probability between 0 and 1. Conceptually, this happened where, in that region, the acoustic impedance and Vp/Vs ratio values fall in the overlapping area of the LFCs. When it happens, the prior probability will have higher impact in the posterior probability equation. This example shows how we should perform training well analysis carefully. Advanced analysis like Rock Physics Template is advised to give better guidance in defining the LFC cluster.

4   CONCLUSIONS

The results show that Bayesian inferences in predicting distribution of lithology could be very useful in development of hydrocarbon field. We provided the full workflow including the statistical aspect in determining prior probability and likelihood function for the lithology of interest that we would like to predict laterally. We can see that limited data could affect the interpretation in reference well and the prior probability estimation. We suggest the reader to incorporate more data, such as water saturation and gamma ray log, as a constraint during the interpretation. Other than that, we blindly classify the lithology class from the cross-plot analysis from three different parameter. Additional method such as Rock Physics Template is advised to give more objective limit between every observed lithology and to give more perspective of porosity and water saturation effect.

References

Aki, K., & Richards, P. (2002). *Quantitative seismology 2nd edn (mill valley, ca.* University Science Books.

Buland, A., Kolbjørnsen, O., Hauge, R., Skjæveland, Ø., & Duffaut, K. (2008, May). Bayesian lithology and fluid prediction from seismic prestack data. *GEOPHYSICS*, *73*(3), C13–C21. Retrieved from https://doi.org/10.1190/1.2842150 doi: doi:10.1190/1.2842150

Buland, A., & Omre, H. (2003, January). Bayesian linearized AVO inversion. *GEOPHYSICS*, *68*(1), 185–198. Retrieved from https://doi.org/10.1190/1.1543206 doi: doi:10.1190/1.1543206

Fatti, J. L., Smith, G. C., Vail, P. J., Strauss, P. J., & Levitt, P. R. (1994, September). Detection of gas in sandstone reservoirs using AVO analysis: A 3-d seismic case history using the geostack technique. *GEOPHYSICS*, *59*(9), 1362–1376. Retrieved from https://doi.org/10.1190/1.1443695 doi: doi:10.1190/1.1443695

Grana, D., Mukerji, T., Dvorkin, J., & Mavko, G. (2012, July). Stochastic inversion of facies from seismic data based on sequential simulations and probability perturbation method. *GEOPHYSICS*, *77*(4), M53–M72. Retrieved from https://doi.org/10.1190/geo2011-0417.1 doi: doi:10.1190/geo2011-0417.1

Grana, D., & Rossa, E. D. (2010, May). Probabilistic petrophysical-properties estimation integrating statistical rock physics with seismic inversion. *GEOPHYSICS*, *75*(3), O21–O37. Retrieved from https://doi.org/10.1190/1.3386676 doi: doi:10.1190/1.3386676

Hampson, D. P., Russell, B. H., & Bankhead, B. (2005, January). Simultaneous inversion of pre-stack seismic data. In *SEG technical program expanded abstracts 2005.* Society of Exploration Geophysicists. Retrieved from https://doi.org/10.1190/1.2148008 doi: doi:10.1190/1.2148008

Kahraman, S., & Yeken, T. (2008, February). Determination of physical properties of carbonate rocks from p-wave velocity. *Bulletin of Engineering Geology and the Environment*, *67*(2), 277–281. Retrieved from

https://doi.org/10.1007/s10064-008-0139-0 doi:
doi:10.1007/s10064-008-0139-0

Krumbein, W. C., & Dacey, M. F.   (1969, March).
Markov chains and embedded markov chains in ge-
ology.   *Journal of the International Association
for Mathematical Geology*, *1*(1), 79–96.   Retrieved
from https://doi.org/10.1007/bf02047072   doi:
doi:10.1007/bf02047072

Larsen, A. L., Ulvmoen, M., Omre, H., & Buland, A.
(2006, September). Bayesian lithology/fluid prediction
and simulation on the basis of a markov-chain prior
model. *GEOPHYSICS*, *71*(5), R69–R78. Retrieved
from https://doi.org/10.1190/1.2245469   doi:
doi:10.1190/1.2245469

Simmons, J. L., & Backus, M. M.   (1996, November).
Waveform-based AVO inversion and AVO prediction-
error. *GEOPHYSICS*, *61*(6), 1575–1588. Retrieved
from https://doi.org/10.1190/1.1444077   doi:
doi:10.1190/1.1444077

Xu, S., & Payne, M. A. (2009, January). Modeling elas-
tic properties in carbonate rocks. *The Leading Edge*,
28(1), 66–74. Retrieved from https://doi.org/10
.1190/1.3064148 doi: doi:10.1190/1.3064148

Zhao, L., Geng, J., Cheng, J., hua Han, D., & Guo, T.
(2014, September). Probabilistic lithofacies predic-
tion from prestack seismic data in a heterogeneous
carbonate reservoir.   *GEOPHYSICS*, *79*(5), M25–
M34.   Retrieved from https://doi.org/10.1190/
geo2013-0406.1 doi: doi:10.1190/geo2013-0406.1